EPR spectroscopic characterization of the iron–sulphur proteins and cytochrome *P*-450 in mitochondria from the insect *Spodoptera littoralis* (cotton leafworm)

Jas K. SHERGILL,*‡ Richard CAMMACK,* Jian-Hua CHEN,† Michael J. FISHER,† Steve MADDEN† and Huw H. REES†

* Centre for the Study of Metals in Biology and Medicine, King's College, University of London, Campden Hill Road, London W8 7AH, and
† Department of Biochemistry, University of Liverpool. P.O. Box 147, Liverpool L69 3BX, U.K.

EPR spectroscopy was used to investigate the cytochrome *P*-450-dependent steroid hydroxylase ecdysone 20-mono-oxygenase of the cotton leafworm (*Spodoptera littoralis*) and the redox centres associated with membranes from the fat-body mitochondrial fraction. Intense features at $g = 2.42$, 2.25 and 1.92 from oxidized mitochondrial membranes have been assigned to the low-spin haem form of ferricytochrome *P*-450, probably of ecdysone 20-mono-oxygenase. High-spin cytochrome *P*-450 (substrate-bound) was tentatively assigned to a signal at $g = 8.0$, which was detectable from membranes as prepared. An EPR signal characteristic of a [2Fe-2S] cluster detected from the soluble mitochondrial matrix fraction has been shown to be distinct from the signals associated with mitochondrial NADH dehydrogenase and succinate dehydrogenase, and has therefore been attributed to a ferredoxin. We conclude that the *S. littoralis* fat-body mitochondrial electron-transport system involved in steroid 20-hydroxylation comprises both ferredoxin and cytochrome *P*-450 components, and thus resembles the enzyme systems of adrenocortical mitochondria. EPR signals characteristic of the respiratory chain were also observed from fat-body mitochondria and assigned to the iron–sulphur clusters associated with Complex I (Centres N1, N2), Complex II (Centres S1, S3), Complex III (the Rieske centre), and the copper centre of Complex IV, demonstrating similarities to mammalian mitochondria. The reduced membrane fraction also yielded a major resonance at $g = 2.09$ and 1.88 characteristic of the [4Fe-4S] cluster of electron-transferring flavoprotein:ubiquinone oxidoreductase. As the fat-body is the major metabolic organ of insects, this protein is presumably required for the β-oxidation of fatty acids in mitochondria. High-spin haem signals in the low-field region of spectra also demonstrated that the mitochondrial fraction contains relatively high concentrations of catalase.

INTRODUCTION

Moulting in insects is controlled by the insect moulting hormones, the ecdysteroids [1]. The prothoracic glands of larvae of the majority of investigated insect species synthesize ecdysone, which is released into the haemolymph [2,3]. Ecdysone undergoes 20-hydroxylation in various peripheral tissues, including fat-body, Malpighian tubules and midgut, yielding 20-hydroxyecdysone, which is generally much more hormonally active and is considered to be the true moulting hormone in most species. This 20-hydroxylation reaction is catalysed by ecdysone 20-mono-oxygenase [ecdysone,hydrogen donor:oxygen oxidoreductase (20-hydroxylating), EC 1.14.99.22]. This protein has been reported to be either largely mitochondrial or microsomal (endoplasmic reticulum), or to have dual location in both subcellular fractions depending upon tissue and species [4,5].

In vertebrates, steroid hydroxylations are mediated by complex enzyme systems referred to as hydroxylases, mono-oxygenases or mixed-function oxidases, which are located in the mitochondria or endoplasmic reticulum of specific tissues or organs such as adrenal cortex, testis, ovary and kidney [6–9]. It is noteworthy that the vertebrate adrenocortical steroid C-20 hydroxylase has a mitochondrial location [10,11]. Ecdysone 20-mono-oxygenase in the fat-body of the cotton leafworm (*Spodoptera littoralis*), the subject of the present paper, is also primarily mitochondrial [12].

The ecdysone 20-mono-oxygenase electron-transport system is cytochrome *P*-450-dependent [5]. In mammals, the electron-transport chains associated with mitochondrial and microsomal steroid hydroxylations differ. Typical mitochondrial systems, for example, adrenocortical mitochondria [13,14] and the *Pseudomonas putida* microbial system [15], consist of an FAD-containing NADPH:ferredoxin reductase (e.g. adrenodoxin reductase), a ferredoxin (a non-haem iron–sulphur protein; e.g. adrenodoxin) and a terminal oxidase, cytochrome *P*-450 [16]. The microsomal systems do not contain a ferredoxin; instead, the reductase possesses an additional FMN molecule which presumably serves a similar function [17].

The optical absorption and EPR properties of vertebrate mitochondrial and microsomal cytochrome *P*-450 have been well characterized [18,19]. The oxidized ferric form of cytochrome *P*-450 (i.e. as isolated or *in situ*) is paramagnetic and is thus detectable by EPR spectroscopy. The rhombic EPR spectrum of substrate-free cytochrome *P*-450 is that of a low-spin ($S = \frac{1}{2}$) ferric haem compound with *g*-values in the $g = 2$ region [20]. The substrate-bound form exhibits an EPR spectrum in the $g = 8$ region characteristic of high-spin ferric haem, which is reducible by NADPH. NADPH is required as a source of electrons by the substrate-specific mono-oxygenase systems. Iron–sulphur proteins are also detectable by EPR spectroscopy; for example, the presence of the [2Fe-2S] ferredoxin, adrenodoxin, purified from

Abbreviations: ETF, electron-transferring flavoprotein; SDH, succinate dehydrogenase; SMP, submitochondrial particles; TMPD, *NNN'N'*-tetramethyl-*p*-phenylenediamine; UQ, ubiquinone.

‡ To whom correspondence should be addressed.

adrenocortical mitochondria was first suggested by an EPR signal at $g = 2.02, 1.94$ [21]. Low-temperature EPR spectroscopy has also been successfully employed for the detection of the iron–sulphur clusters of mitochondrial Complex I (NADH dehydrogenase, Centres N1–N4), Complex II (succinate dehydrogenase, Centres S1–S3) and Complex III (ubiquinol : cytochrome *c* oxidoreductase, the Rieske centre) of the respiratory chain, together with the cytochromes associated with Complexes III and IV and the copper site of cytochrome aa_3 oxidase [22,23].

On the basis of EPR studies, the occurrence of a ferredoxin serving as an electron-transfer intermediate in fat-body mitochondria of the tobacco hornworm (*Manduca sexta*), has been suggested [24]. Cytochrome *P*-450 was not definitively detected in the EPR study. However, cytochrome *P*-450 has been detected by CO difference spectra in mitochondrial preparations catalysing ecdysone 20-hydroxylation in various species (for a review, see [25]). In the case of fat-body mitochondria from *M. sexta*, a photochemical action spectrum of reversal of CO inhibition of ecdysone 20-mono-oxygenase displayed a maximum at 450 nm [24,26], and established the role of cytochrome *P*-450 as a biocatalyst in the C-20 hydroxylation of ecdysone. Nevertheless, as there has only been preliminary application of the EPR technique to the study of insect systems [24], there is a lack of information on the individual components of the insect mitochondrial ecdysone 20-mono-oxygenase electron-transfer system.

Recently, Chen et al. [27] demonstrated that antibodies raised against bovine adrenal cytochrome *P*-450scc, cytochrome *P*-$450_{11\beta}$, adrenodoxin and adrenodoxin reductase effectively inhibited *S. littoralis* fat-body mitochondrial ecdysone 20-mono-oxygenase activity, thereby suggesting that this hydroxylating system may contain polypeptide components analogous to those in vertebrate steroid hydroxylase systems. In order to establish whether the insect system resembles that of vertebrate mitochondrial or microsomal steroid hydroxylation electron-transfer chains, we have investigated the ecdysone 20-mono-oxygenase system of *S. littoralis* using EPR spectroscopy. In the present paper we also report on the EPR-detectable iron–sulphur and haem proteins, which characterize the respiratory system of *S. littoralis* fat-body mitochondria.

EXPERIMENTAL

Materials

All chemicals were of the purest quality available. Ecdysone was a gift from Dr. G. B. Russell, D.S.I.R., Palmerston North, New Zealand. A solution of ethanol containing ecdysone (5.0 μg) was evaporated to dryness under nitrogen in a glass vial, and the dry film obtained re-dissolved by vortex-mixing with 50 μl of 50 mM sodium Hepes, pH 7.0.

Animals

Last-instar *S. littoralis* larvae were reared on an artificial diet under a photoperiod of 18 h light:6 h dark at 28 °C and 70% relative humidity, as described previously [27].

Preparation of mitochondria of fat-body tissue from *S. littoralis* larvae

The fat-bodies from the last-instar larvae were dissected and homogenized using a Potter–Elvejem homogenizer as described previously [27]. The mitochondrial fraction was prepared by differential centrifugation (10000 *g* for 15 min), as described by Hoggard and Rees [12], and resuspended in Buffer A (250 mM sucrose/10 mM sodium Hepes/1 mM $MgCl_2$/1 mM Na-ATP/5 mM sodium succinate/0.2 mM NADH/1 mM EDTA/0.1 mM dithiothreitol, pH 7.1). Typical preparations had an ecdysone 20-mono-oxygenase activity of 14.6 ± 2.9 pmol/min per mg of protein.

Preparation of mitochondrial membranes

As EPR experiments require high protein concentrations, mitochondria were converted into submitochondrial membrane particles (SMP) by sonication. Mitochondria were thawed, diluted to a protein concentration of ~ 10 mg/ml with Buffer A, and centrifuged at 27000 *g* for 10 min. The pellet was resuspended to ~ 20 mg of protein/ml in Buffer A, and 3 ml aliquots were sonicated in an ice bath with eight separate 15 s bursts (with 15 s intervals) with a microtip probe. The sonicated suspension was centrifuged at 27000 *g* for 10 min and, without disturbing the lower mitochondrial pellet, the supernatant was removed and stored at 4 °C. The pellet was then resuspended, sonicated and re-centrifuged as described above, and then the supernatant was combined with the original supernatant fraction and centrifuged at 130000 *g* for 1 h. The viscous brown pellet was washed in Buffer B (250 mM sucrose/50 mM sodium Hepes/1 mM EDTA/0.1 mM dithiothreitol, pH 7.5) and re-centrifuged at 130000 *g* for 1 h. The final SMP pellet was resuspended in a minimal volume of Buffer B, to a protein concentration of 25 mg/ml (unless otherwise stated in the Figure legends). The supernatant fraction, which contains the soluble matrix enzymes, was concentrated to a protein concentration of 7.1 mg/ml.

SMP samples (150–200 μl) were transferred to quartz EPR tubes (~ 3 mm internal diameter). All additions were made to the EPR tube via long-needled syringes, under a steady stream of argon gas. For the formation of high-spin cytochrome *P*-450, some oxidized SMP preparations were treated with an excess of the substrate, ecdysone (10 μM; $K_m = 0.5$ μM for ecdysone 20-mono-oxygenase), for 10 min. To confirm the presence of catalase, some preparations were treated with 10 mM sodium formate for 10 min. The redox state of the mitochondrial iron–sulphur clusters was adjusted by the addition of either 4 mM NADPH, 30 mM succinate or 2 mM dithionite, samples being incubated for 2, 30 and 2 min respectively. Prior to reduction of SMP with succinate, the sample was treated with 5 mM $MgCl_2$/25 μM ATP/25 μM KH_2PO_4 in order to activate mitochondrial succinate dehydrogenase (SDH), as described previously [28,29]. Concentrated preparations (~ 15 mg total protein) were obtained for the specific observation of the Rieske [2Fe-2S] cluster of mitochondrial Complex III, by centrifugation at 27000 *g* for 15 min in quartz EPR tubes, using Perspex (Lucite) blocks machined to fit a Sorvall 8 × 50 ml (SS34) rotor [30]. The membranes were then selectively reduced with 10 mM ascorbate and 100 μM TMPD for 30 min at 25 °C, under an argon atmosphere. After reduction, all samples were frozen at 77 K.

X-band EPR spectra were recorded on a Bruker ESP300 spectrometer fitted with a TE102 rectangular cavity, a Hewlett–Packard 5350B microwave frequency counter and an Oxford Instruments ESR900 liquid-helium-flow cryostat. Spectral baselines were corrected by subtraction of a cavity/water spectrum recorded under identical conditions.

RESULTS

The $g = 2$ region of the EPR spectra of *S. littoralis* mitochondrial membranes

Figure 1 shows the $g = 2$ region of the EPR spectra of *S. littoralis* fat-body mitochondrial membranes, as prepared (i.e. oxidized).

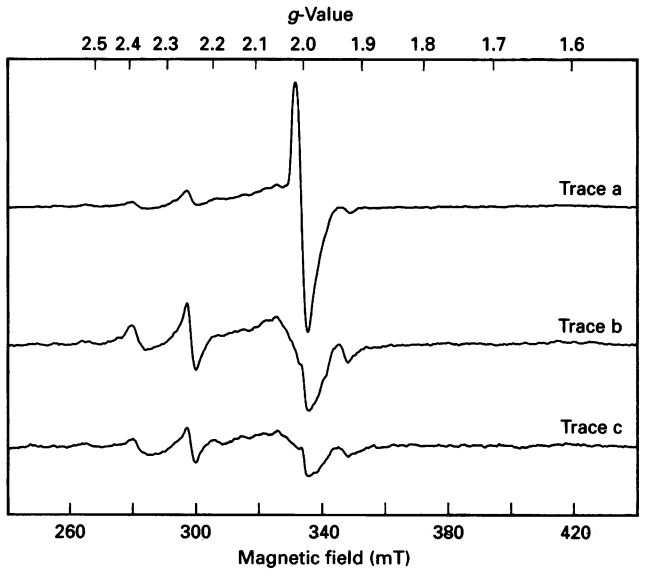

Figure 1 The $g = 2$ region of the EPR spectra of oxidized *S. littoralis* fat-body mitochondrial membranes, recorded at 8 K (trace a), 30 K (trace b) and 60 K (trace c)

Measurement conditions were: microwave power, 20 mW; microwave frequency, 9.38 GHz; modulation amplitude, 1.0 mT; time constant, 0.33 s; sweep rate, 2.4 mT/s. The spectra are an average for four scans.

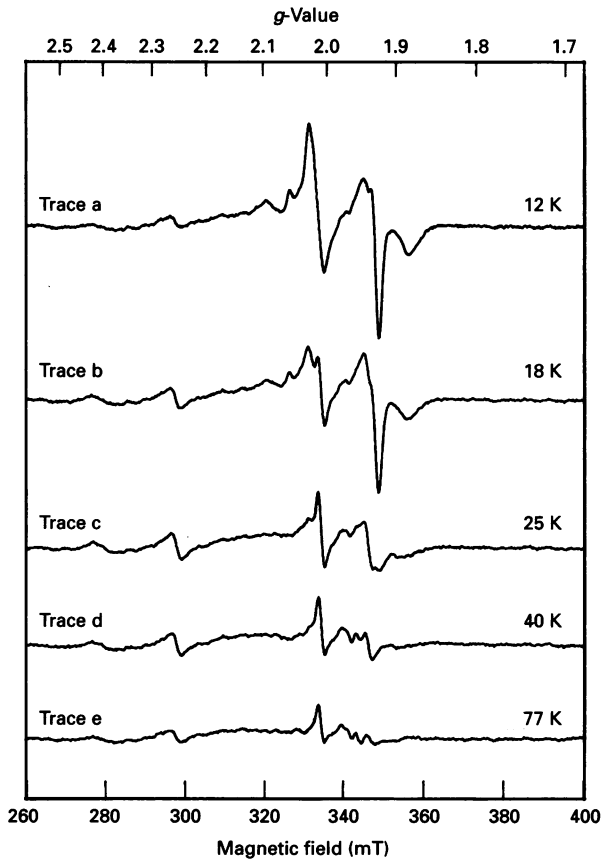

Figure 2 Temperature-dependence of the EPR spectra of reduced *S. littoralis* fat-body mitochondrial membranes

Membranes were reduced with 4 mM NADPH as described in the Experimental section. Measurement conditions were as for Figure 1, except for the following: time constant, 0.08 s; sweep rate, 1.2 mT/s.

At 8 K the membranes exhibited an intense narrow signal at $g = 2.015$ (Figure 1, trace a) characteristic of the oxidized [3Fe-4S] cluster of mitochondrial SDH Centre S3. This signal was detected between 6 and 21 K only; at higher temperatures, this signal disappeared and an axial signal emerged at $g = 2.016, 2.15$ from the copper-A centre of cytochrome aa_3 oxidase (Figure 1, traces b and c). This latter signal was also detectable to a lower temperature, as observed previously with membranes of mammalian mitochondria [31].

The other major features in the spectrum (Figure 1), at $g = 1.923$, 2.251 and 2.421, are assigned to the low-spin haem form of ferricytochrome *P*-450. This signal was clearly detectable up to 77 K. Low-spin cytochrome *P*-450 characteristically exhibits an EPR signal at $g \sim 1.9$, 2.2 and 2.4 [20], whilst high-spin cytochrome *P*-450 displays features at $g \sim 1.7$, 3.7 and 8 (see the next subsection).

Treatment of the membranes with 4 mM NADPH resulted in a decrease in intensity of both the $g = 2.015$ feature and the signal assigned to low-spin cytochrome *P*-450 (Figure 2). The residual $g = 2.015$ signal observed at 12 K in NADPH-reduced membranes indicates that some of the [3Fe-4S] cluster of SDH Centre S3 was not accessible to reductant (Figure 2, trace a). New EPR signals typical of a number of reduced [2Fe-2S] and [4Fe-4S] clusters were noted, overlapping in the $g = 2$ region. Some of these features are characteristic of the highly conserved lineshapes of mitochondrial NADH dehydrogenase (Complex I) Centres N1 and N2. Whilst the g_{xy} feature of the [2Fe-2S] cluster of Centre N1 is clearly resolved at $g = 1.94$ at 12 K (Figure 2, trace a), the g_z feature is superimposed on the dominating $g = 2.015$ signal from SDH Centre S3 and therefore not resolved. The $g_z = 2.02$ feature of Centre N1 was, however, resolved at higher temperature (e.g. 18 K), despite overlap from a free-radical signal at $g \sim 2.004$ (Figure 2, trace b). The distinct EPR signal of the [4Fe-4S] cluster of Centre N2 at $g_z = 2.05$, $g_{xy} = 1.92$, was detected only at temperatures below 25 K, which is typical behaviour for this cluster (Figure 2, traces a and b). The lineshape and temperature-dependence of this signal are very distinctive and serve as a good diagnostic test for the presence of NADH dehydrogenase (Table 1).

To both low- and high-field of the NADH dehydrogenase signals is another rhombic EPR signal with prominent features at $g = 2.09$ and 1.88. This signal was observed only with membranes in the reduced state (compare Figures 1 and 2) and at temperatures below 20 K. We attribute the $g = 2.09$ and 1.88 features to the [4Fe-4S] cluster of the mitochondrial electron-transferring flavoprotein (ETF):ubiquinone (UQ) oxidoreductase, as the signal displays the spectral characteristics and temperature-dependence of this cluster. The expected third *g*-value from this cluster, which corresponds to $g_y = 1.94$, is obscured by the signal from Centre N1. This protein transfers electrons from fatty-acyl-CoA dehydrogenases to the respiratory chain at the level of UQ in mammalian mitochondria [32]. Previous EPR studies have shown the protein to comprise a [4Fe-4S] cluster and FAD [32,33]. An isotropic EPR signal at $g = 2.003$ from the semiquinone form of FAD has been detected from pig liver ETF:UQ oxidoreductase [33]. It seems possible, therefore, that the free radical detected at $g \sim 2.004$ at higher temperatures in NADPH-reduced membranes is due to the FAD-anionic semiquinone species (Figure 2, traces b–e).

Table 1 Characterization and assignment of the EPR signals from *S. littoralis* mitochondrial membranes

g-Value	Redox state	Centre	Assignment
$g = 2$ region			
2.01	Oxidized	[3Fe-4S]	Succinate dehydrogenase Centre S3 (Complex II)
2.018, 2.15	Oxidized	Cu^{2+}	Cytochrome aa_3 oxidase (Complex IV)
1.92, 2.25, 2.42	Oxidized	Fe^{3+}, low-spin haem	Cytochrome *P*-450
1.94, 2.02	Reduced	[2Fe-2S]	NADH dehydrogenase Centre N1 (Complex I), Succinate dehydrogenase Centre S1 (Complex II)
1.92, 2.05	Reduced	[4Fe-4S]	NADH dehydrogenase Centre N2 (Complex I)
1.88, 2.09	Reduced	[4Fe-4S]	ETF:UQ oxidoreductase
1.76, 1.895	Reduced	[2Fe-2S] 'Rieske'	Ubiquinol:cytochrome *c* oxidoreductase (Complex III)
Low-field region			
3.01	Oxidized	Fe^{3+}, low-spin haem	Cytochrome aa_3 oxidase (Complex IV)
3.4	Oxidized	Fe^{3+}, low-spin haem	Cytochrome *b* and *c* (Complex III, see the text)
4.3	Oxidized	Fe^{3+}, high-spin	Mononuclear non-haem iron
6.34, 5.46	Oxidized	Fe^{3+}, high-spin haem	Catalase A
6.86, 5.08	Oxidized	Fe^{3+}, high-spin haem	Catalase B
8.04	Oxidized	Fe^{3+}, high-spin haem	Cytochrome *P*-450, substrate-bound

The EPR spectrum observed with succinate-reduced membranes was essentially identical with that obtained with NADPH-reduced membranes (see Figure 2). However, treatment with succinate resulted in the total disappearance of the [3Fe-4S] cluster signal at 12 K, indicating total reduction of SDH Centre S3. In the case of succinate-reduced SMP, it is likely that the appearance of a signal at $g_z = 2.02$ and $g_{xy} = 1.94$ was due to reduction of the [2Fe-2S] cluster of SDH Centre S1. However, as a signal at $g_z = 2.05$, $g_{xy} = 1.92$ was also detected, it is clear that reduction of NADH dehydrogenase Centre N2 had also occurred. It seems likely, therefore, that the succinate-mediated reduction of the $g_z = 2.05$, $g_{xy} = 1.92$ features indicates reverse electron-flow from a common electron acceptor, in this case, UQ. If so, it is probable that the signal at $g_z = 2.02$ and $g_{xy} = 1.94$ contains contributions from the [2Fe-2S] clusters of both reduced Centres N1 and S1 (see Table 1). Similar spectra were also observed on reduction with dithionite, although the intensities of the reduced iron–sulphur clusters were markedly increased, in contrast with the features due to low-spin cytochrome *P*-450 (see Figure 2).

In an EPR investigation of fat-body mitochondria from *M. sexta*, Smith et al. [24] assigned a signal with features at $g = 2.014$ and 1.942 to a [2Fe-2S] cluster of a ferredoxin associated with a mitochondrial steroid-hydroxylation system, implying similarities to vertebrate systems. We have been unable to confirm the presence of ferredoxin in *S. littoralis* fat-body mitochondrial membranes by EPR spectroscopy. Although we have observed a similar EPR signal typical of a [2Fe-2S] cluster at $g = 2.02$ and 1.94 (Figure 2), our studies show that this signal is most likely due, at least in part, to Centre S1 of mitochondrial SDH, for it is observed upon reduction with either succinate or dithionite, and the detection of a $g = 2.01$ signal in oxidised SMP preparations has provided evidence for the presence of SDH. In order to resolve this issue, we have studied the power-saturation profiles of the signal in question. Figure 3(a), a plot of (normalized signal intensity/$\sqrt{\text{power}}$) versus microwave power, compares the power-saturation characteristics of succinate- and dithionite-reduced mitochondrial membranes. Under non-saturating conditions, such plots should be horizontal straight lines with the onset of power saturation marked by a downward deviation from linearity. At 30 K, the $g = 1.94$ feature from succinate-reduced membranes is characterized by a $P_{\frac{1}{2}}$ of ~ 0.3 mW. The spin-relaxation rate of the species giving rise to the feature is enhanced upon dithionite reduction, $P_{\frac{1}{2}} \sim 1.5$ mW (Figure 3a); this relief in the microwave power saturation of the [2Fe-2S] cluster is believed to be brought about by the presence of a third iron–sulphur centre which becomes paramagnetic only after reduction with a strong reductant such as dithionite. This unusual phenomenon has been observed for several preparations of SDH [34], where the increase in the relaxation rate observed for the $g = 1.94$ feature has been attributed to spin-coupling between the [2Fe-2S] cluster of Centre S1 and the [4Fe-4S] cluster of Centre S2, the third iron–sulphur cluster of SDH [35]. We can therefore assign the $g_{z,yx} = 2.02$, 1.94 axial EPR signal from reduced fat-body mitochondrial membranes to SDH Centre S1.

Reduction of the mitochondrial membranes with ascorbate and TMPD led to preferential reduction of the Rieske [2Fe-2S] cluster (Figure 4). The characteristic rhombic 'Rieske' EPR signal was first observed for Complex III of mammalian mitochondria ($g_{zyx} \sim 2.03$, 1.90 and 1.78) [36]. The signal observed at 20 K from the reduced Rieske cluster of fat-body mitochondria displays features at $g_{yx} = 1.895$ and 1.76 (Figure 4, trace a; see the '$\times 5$' inset). The g_z feature of the Rieske cluster is difficult to observe, due to overlap from the $g = 2.015$ signal of SDH Centre S3 at low temperatures ($\leqslant 21$ K), and the appearance of a new broad signal at $g = 2.08$ at higher temperatures ($\geqslant 25$ K) (Figure 4, trace b), which we have assigned to a nitrosyl–haem complex. The triplet hyperfine structure observed at $\geqslant 30$ K superimposed upon the broad feature at $g \sim 2$ (Figure 4, trace b) is broadened out by microwave power saturation at temperatures below 25 K ($A \sim 1.7$ mT). The origin of this signal is at present unknown, although it probably contains contributions from both catalase (see below) and cytochrome *P*-420.

Thus far it appears that the EPR signals in the $g = 2$ region can be interpreted by analogy to mammalian mitochondria [37,38]. The results are entirely consistent with assignment to the metallocentres of NADH dehydrogenase, SDH, ubiquinol: cytochrome *c* oxidoreductase and cytochrome aa_3 oxidase (mitochondrial Complexes I, II, III and IV respectively), in their normal proportions.

The high-spin haem signals from *S. littoralis* mitochondrial membranes

Signals were also observed in the low-field region of the EPR spectra of *S. littoralis* membranes; for example, the membrane

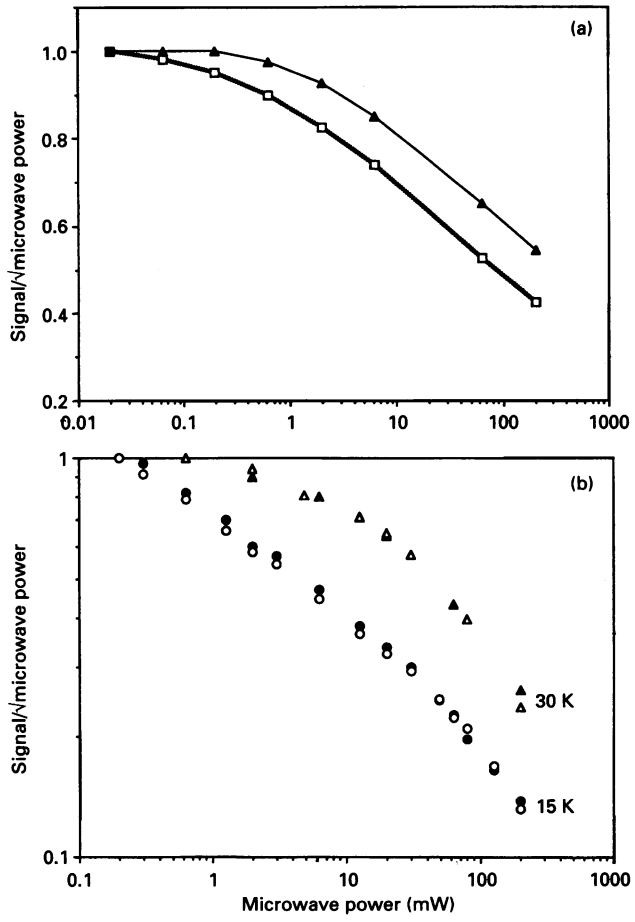

Figure 3 Power-saturation profile of the EPR $g = 1.94$ feature observed from succinate- and dithionite-reduced *S. littoralis* fat-body mitochondrial fractions

(**a**) Membranes (□, succinate; ▲, dithionite); (**b**) matrix fraction (●, ▲, dithionite; ○, △, succinate). The signal amplitude was determined using the peak-to-trough height of the first derivative signal at $g \sim 1.94$ following a baseline subtraction. The signal sizes were normalized so that, at low microwave powers, they had identical values of signal/$\sqrt{}$microwave power. EPR-signal-measurement conditions were as for Figure 1, except for the following: microwave frequency, 9.35 GHz; time constant, 0.08 s; sweep rate, 0.60 (**a**), 0.72 (**b**) mT/s; temperature, 30 (**a**), 15 and 30 K (**b**); number of scans, 4 (**a**) and 5 (**b**).

fraction as prepared (Figure 5, trace a) displayed a rather intense high-spin ferric haem signal at $g = 6.0$, and a rhombic non-haem ferric iron signal at $g = 4.3$. Furthermore, other features on either side of the feature at $g = 6.0$ could also be detected, at $g \sim 6.33$, 5.45. We provisionally assign these features to active catalase A high-spin haem, for the following reasons: (a) the g-values are very similar to those of isolated rat liver, bovine liver and human erythrocyte catalase, and (b) the spectrum could be modified by the addition of formate (see Figure 6b), which is a peroxidative substrate for catalase, binding to the enzyme as the free acid to give catalase B ($g \sim 6.8$, 5.0) [39].

A closer examination of the low-field side of the spectrum of oxidized membranes also revealed EPR signals at $g \sim 6.6$, 6.9 and 8.04 (Figure 5, trace a). A signal at $g \sim 8$ is expected from the high-spin form of cytochrome *P*-450. This protein is expected to convert from the low-spin ferric form, which displays features in the $g = 2$ region (see Figure 1), to the high-spin ferric form on formation of an enzyme–substrate complex. However, the spectrum of Figure 1(b) was unchanged on ecdysone addition.

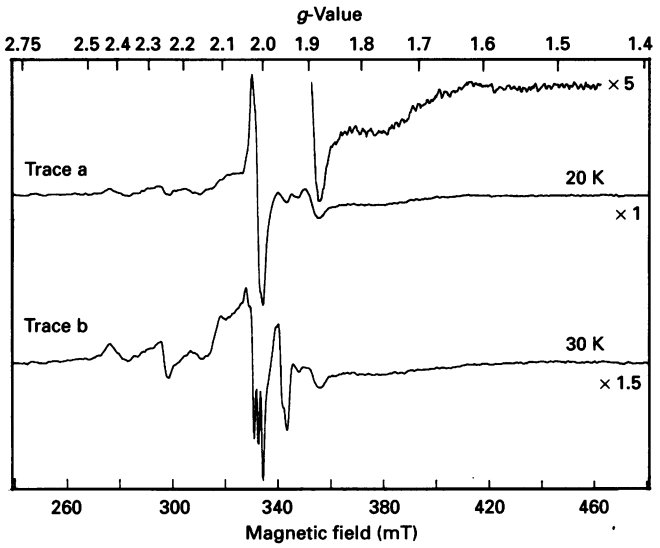

Figure 4 EPR spectra of ascorbate/TMPD-reduced *S. littoralis* fat-body mitochondrial membranes

Measurement conditions were as for Figure 1, except for the following: microwave frequency, 9.36 GHz; time constant, 0.08 s; sweep rate, 1.2 mT/s. The protein concentration was ~ 100 mg/ml. The spectra are an average for ten scans. Traces a and b are described in the text.

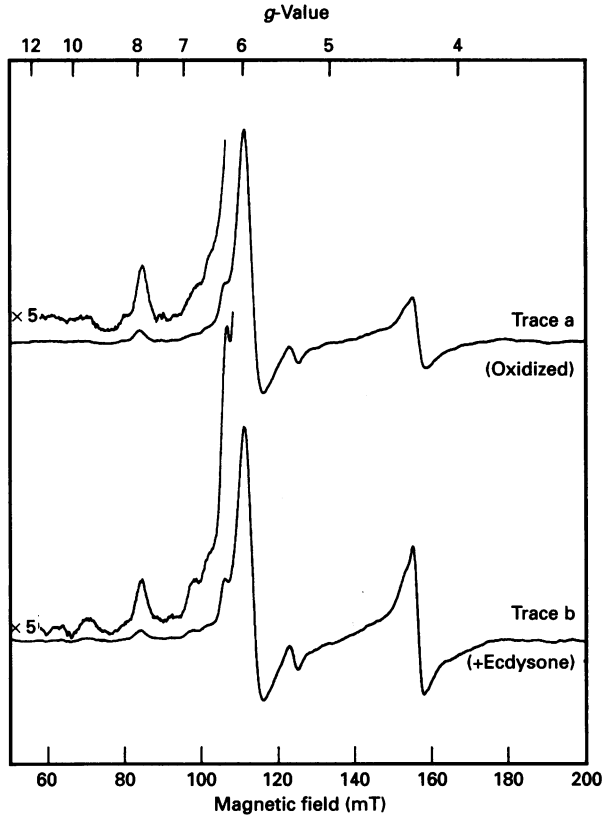

Figure 5 A comparison of the high-spin cytochrome *P*-450 EPR signals from *S. littoralis* fat-body mitochondrial membranes as prepared and treated with ecdysone

Measurement conditions were as for Figure 1, except for the following: microwave frequency, 9.35 GHz; time constant, 0.08 s; sweep rate, 0.9 mT/s; temperature, 6 K. The spectra are an average for ten scans.

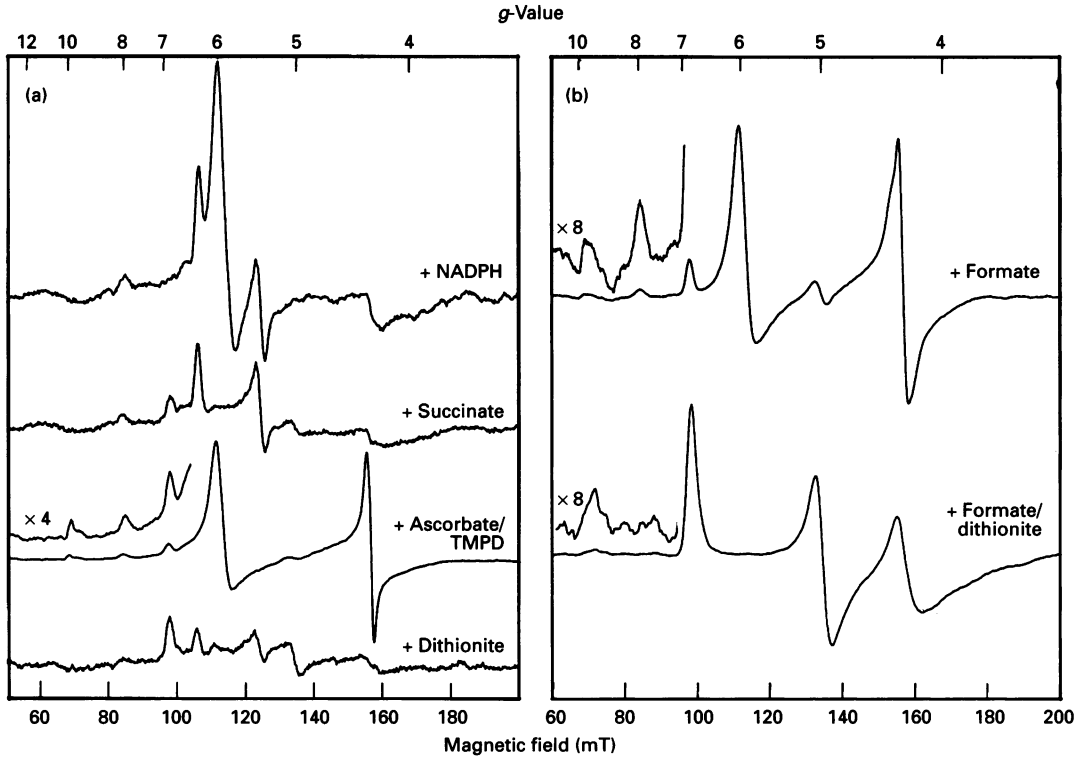

Figure 6 Low-field region of the EPR spectra of reduced (a) and formate-treated (b) *S. littoralis* fat-body mitochondrial membranes

Measurement conditions were as for Figure 1, except for the following: microwave frequency, 9.38 (**a**) and 9.36 (**b**) GHz; time constant, 0.08 s; sweep rate, 0.9 (**a**) and 1.2 (**b**) mT/s; temperature, 6 K. Protein concentration of the ascorbate/TMPD treated sample, ~ 100 mg/ml; all other samples, 25 mg/ml. Spectra are an average for ten scans.

Furthermore, no significant change in the intensity of the $g = 8.0$ signal was observed on incubation of the membranes with the substrate for 20-hydroxylation, ecdysone, in excess quantities (Figure 5, trace b). As there appears to be no concomitant decrease in intensity of the low-spin haem-*P*-450 features on addition of ecdysone, and no new features detectable in the low-field region of the EPR spectrum, we conclude that, if cytochrome *P*-450 is present in the membranes, as prepared, it is already ecdysone-bound.

On reduction of the membranes with NADPH, the signal assigned to high-spin cytochrome *P*-450 ($g = 8.04$) decreased in intensity, as would be expected upon electron transfer from NADPH via an NADPH:ferredoxin reductase to the terminal oxidase, cytochrome *P*-450 (Figure 6a). However, the catalase EPR signals now appear to be more prominent. It is also worth noting that a minor signal could now be detected at $g \sim 8.4$. Williams-Smith and Patel [39] have also noted features in the $g = 8$ region using high concentrations of either bovine or rat liver catalase, and assigned a signal at $g = 8.52$ to rhombically distorted haem. Treatment with either succinate, ascorbate/TMPD or dithionite resulted in similar spectra containing contributions from both catalases A and B, although the intensities of the two species are clearly different, with catalase A still dominating the low-field region of succinate-reduced membranes (Figure 6a). The shift in the *g*-values provisionally assigned to catalase A , to $g = 6.8$ and 5.0, on treatment of mitochondrial membranes with formate, is typically observed upon formation of the catalase–formate complex, catalase B, and is probably due to a change in the rhombicity of iron (Figure 6b) [39]. Reduction of the formate-treated sample resulted in the total disappearance of the $g = 6.0$ haem EPR signal, thereby enhancing the features due to catalase B, which is only slowly reduced by dithionite (Figure 6b).

EPR spectra of *S. littoralis* fat-body microsomes were also recorded, and no signals due to either catalase A or B, or cytochrome *P*-450, observed (results not shown). The haem-*P*-450 results are consistent with the observations of Hoggard and Rees [12], who demonstrated that most of the ecdysone 20-mono-oxygenase activity is mitochondrial, with only a small amount associated with the microsomal fraction. Microsomal xenobiotic-metabolizing *P*-450s would also be expected, but in this case are likely to be present at only low levels in the absence of appropriate inducing agents. The catalase may represent contamination of the mitochondrial membrane fraction by peroxisomes, cytoplasmic microbodies rich in catalase [40].

Other low-spin haem signals were resolved in the $g = 3$ region of the wide-scan EPR spectrum from oxidised *S. littoralis* membranes, at $g \sim 3.01$, 3.25 and 3.4 (Figure 7). By analogy to the EPR signals from the cytochromes of the mammalian mitochondrial respiratory chain, we assign these features to cytochrome aa_3 oxidase ($g \sim 3.01$), and cytochromes c_1 and b_{562} ($g \sim 3.4$) [41–43].

As yet, our EPR analysis of the *S. littoralis* mitochondrial membranes has provided no conclusive evidence for an EPR signal analogous to that observed from adrenodoxin with vertebrate adrenocortical steroid-hydroxylation systems (see Figure 2). Adrenodoxin is known to be loosely bound to the adrenal-cortex mitochondrial membranes and can be readily detached from the membrane during sonication [44]. The possibility that the *S. littoralis* mono-oxygenase system comprises a ferredoxin,

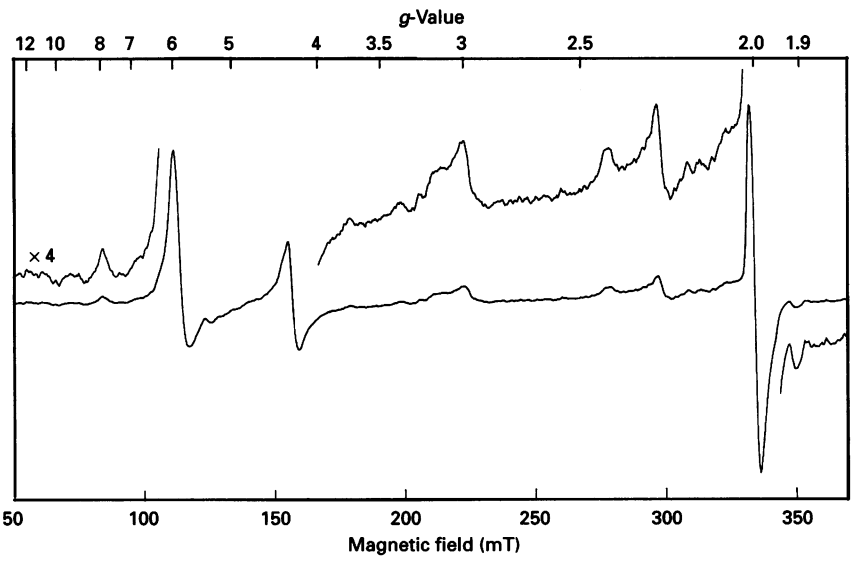

Figure 7 Wide-scan EPR spectrum of oxidized *S. littoralis* fat-body mitochondrial membranes recorded at 12 K

The spectrum is an average for five scans. Other measurement conditions were as for Figure 1.

which has washed away from the mitochondrial membranes and is now located in the matrix fraction, is investigated in the next section.

The EPR signals from the *S. littoralis* mitochondrial matrix fraction

The soluble mitochondrial matrix fraction, in the oxidized state, also displayed high-spin haem signals characteristic of both catalases A and B, and a non-haem signal from mononuclear ferric iron (Figure 8a); a high-spin ferric haem signal at $g = 6$ was not detected. As was observed previously, the ratio of the catalase A and B features changed markedly upon the addition of dithionite, the former species being barely detectable after reduction.

In the high-field region of the 10 K EPR spectrum from the oxidized matrix fraction, a signal displaying the characteristics of a [3Fe-4S] cluster was observed at $g \sim 2.02$ (Figure 8b). The distinctive lineshape of this signal, which disappears at temperatures above 35 K (see the upper spectrum in Figure 8c), appears to consist of two components, the first giving rise to a peak at $g = 2.026$, and the second to a feature centred at $g \sim 2.008$. Treatment with dithionite resulted in the complete disappearance of this signal. Ruzicka and Beinert [45] have observed an identical signal from the soluble iron–sulphur protein aconitase located in the matrix fraction of the mitochondrion. The aconitase EPR signal has been shown to consist of two similar components that differ slightly in their redox potentials; the ratio of these components has also been shown to vary in different preparations [45].

It should perhaps be noted that the hydrophilic iron–sulphur subunit of SDH is anchored to the mitochondrial membrane by two small hydrophobic peptides. It is therefore possible that, during SMP preparation by sonication, some of the iron–sulphur subunit may have become detached from the membrane. If so, the possibility exists that the EPR signal from the oxidized matrix fraction may represent contributions from the [3Fe-4S] clusters of both SDH Centre S3 and aconitase. However, as the signal from the matrix fraction could be detected up to a temperature of ~ 25 K (Figure 8b), it does not display the temperature-dependence of SDH Centre S3, which is detected below 21 K only. Furthermore, unlike the $g = 2.015$ feature from SDH Centre S3, the $g \sim 2.02$ signal did not decrease in intensity on the addition of succinate, indicating that the [3Fe-4S] cluster giving rise to this signal is not reducible by this substrate. We therefore assign the two-component feature exclusively to aconitase.

At a higher temperature of 40 K, a weak signal characteristic of a [2Fe-2S] cluster is present in the EPR spectrum of the oxidized matrix fraction at $g = 2.02$, 1.94, indicating that the sample is partially reduced (Figure 8c); the latter feature was clearly detected at lower temperatures also (see Figure 8b). Again the possibility exists that the [2Fe-2S] cluster signal represents detection of SDH (Centre S1) detached from the membrane. However, this seems unlikely, as no significant increase in the signal amplitude of the $g = 1.94$ feature was observed upon reduction of the sample with succinate, the substrate for SDH, whilst an approx. 3-fold increase in intensity was noted on reduction with dithionite (Figure 8c). The intense signals observed with the membrane fraction from the reduced [2Fe-2S] and [4Fe-4S] clusters of mitochondrial Complexes I and II were not observed in the EPR spectra recorded with the dithionite-treated matrix fraction over the 8–30 K temperature range.

The microwave-power-saturation characteristics of the $g \sim 1.94$ feature from the succinate- and dithionite-reduced matrix fraction are compared in Figure 3(b). As the EPR signal was very weak at low microwave powers, the saturation behaviour of the signal was not investigated at powers below 0.2 mW. Both samples clearly display similar power-saturation characteristics at 15 K and 30 K. As no relief in power saturation was observed with dithionite (compare with Figure 3a), it is highly unlikely that the EPR signal is due to SDH Centre S1.

A prominent rhombic EPR signal at $g = 2.60$, 2.239 and 1.845 (results not shown, although the latter feature is visible in Figure 8c) was also detected over the 12–40 K temperature range, from the dithionite-reduced matrix fraction. The origin of this signal is as yet unknown, although it appears to display the characteristics of a low-spin haem, and may represent distorted cytochrome *P*-450.

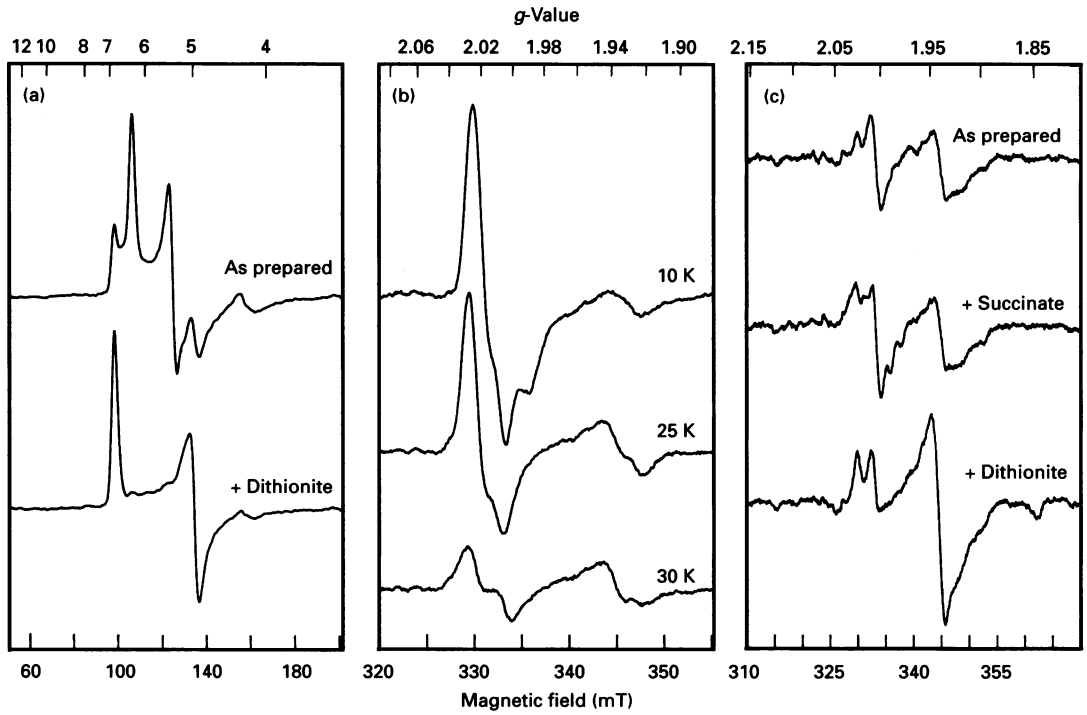

Figure 8 EPR spectra of the matrix fraction from *S. littoralis* fat-body mitochondria

(**a**) Low-field region; (**b**) $g = 2$ region of oxidized fraction; (**c**) $g = 2$ region of the matrix fraction in various redox states. Measurement conditions were as for Figure 1, except for the following: microwave frequency, 9.375 (**a**) and 9.351 (**b** and **c**) GHz; sweep rate, 2.4 (**a**), 0.6 (**b**) and 0.7 (**c**) mT/s; temperature, 6 (**a**), 10, 25 and 30 (**b**) and 40 (**c**) K. Spectra are an average for five (**a**), two (**b**) or four (**c**) scans.

DISCUSSION

Cytochrome *P*-450

The EPR spectra of the *S. littoralis* fat-body mitochondrial membrane fraction exhibited signals characteristic of both low-spin (g_{xyz} = 1.92, 2.25, 2.42) and substrate-bound high-spin (g = 8.0) cytochrome *P*-450. We attribute these signals to mitochondrial ecdysone 20-mono-oxygenase, an NADPH-requiring cytochrome *P*-450-dependent steroid hydroxylase. Essentially similar features have been observed from cytochrome *P*-450 of mammalian tissues. This is the first EPR spectrum reported for the cytochrome *P*-450 component of an invertebrate steroid hydroxylase, although cytochrome *P*-450 has previously been demonstrated in the fat-body mitochondrial fraction from *M. sexta*, using CO difference spectroscopy [26]. The inability to confirm the presence of cytochrome *P*-450 in *M. sexta* fat-body mitochondrial fraction by EPR spectroscopy was attributed to the low concentration of the cytochrome in insect mitochondria when compared with vertebrate adrenal-cortex mitochondria (by a factor of 150) [24].

No change in the EPR signal from cytochrome *P*-450 could be detected upon ecdysone treatment of oxidised mitochondrial membranes; the most feasible explanation at this time is that the membranes, as prepared, already contain substrate-bound haem-*P*-450. A large number of preparations were examined during the course of this work, and all gave rise to similar EPR spectra. That the cytochrome is a functional catalytic component of fat-body ecdysone 20-mono-oxygenase has, nonetheless, been established by a photochemical action spectrum, for *M. sexta* [26]. Both the low- and high-spin forms of cytochrome *P*-450 were reducible by NADPH, presumably due to electron transfer via a NADPH:ferredoxin reductase, as noted by a decrease in intensity of the features in the $g = 2$ region and at $g = 8.0$.

Mitochondrial respiratory-chain components

In the present study we have demonstrated marked similarities in composition between the respiratory chain of *S. littoralis* and mammalian mitochondria [23,31]. The EPR signals assigned to Complexes I, II, III and IV associated with respiratory chains are summarized in Table 1. Intense features characteristic of NADH dehydrogenase Centres N1 and N2 were observed from NADPH-reduced *Spodoptera* mitochondrial membranes. However, the EPR signals associated with the two other [4Fe-4S] clusters of NADH dehydrogenase, Centres N3 and N4, were not observed. These centres normally give rise to relatively weak features at low temperatures ($\leqslant$ 15 K) at $g_{z,yx}$ = 2.08, 1.86 and $g_{z,yx}$ = 2.10, 1.88 respectively [23]. It seems likely that these signals are buried under the major resonances arising from the [4Fe-4S] cluster of ETF:UQ oxidoreductase, at $g = 2.09$ and 1.88.

It is noteworthy that membranes in the reduced state exhibited a signal characteristic of relatively high concentrations of ETF:UQ oxidoreductase. This implies that an ETF-dependent enzyme system may be present in *S. littoralis* fat-body mitochondria, such as for the β-oxidation of fatty acids; indeed the fat-body is the major metabolic organ in insects. The concentration of this protein appears to be particularly low in ox heart [32], and relatively high in pigeon heart, breast muscle and, particularly, brown adipose tissue, which is highly specialized for fatty acid oxidation [37,46,47].

ETF:UQ oxidoreductase can accept a maximum of three electrons; one electron for reduction of the [4Fe-4S] cluster, and

two for full reduction of the FAD moiety. It has been suggested that the electron acceptor may be UQ, or UQ tightly associated with mitochondrial Complex III [48]. Although the EPR signals characteristic of the [4Fe-4S] cluster and the FAD-anionic semiquinone were observed after reduction with dithionite, the same signals represented a major contribution to the spectra from either NADPH- or succinate-reduced membranes. However, these signals were not observed upon use of the chemical reductant ascorbate/TMPD. Similar results have been obtained with pigeon heart SMP [37] and *Paracoccus denitrificans* [31]. It appears, therefore, that the [4Fe-4S] cluster of ETF:UQ oxidoreductase equilibrates with both Complexes I and II of the respiratory chain. This could be achieved via a mobile UQ pool and reverse electron flow from ubiquinol to ETF:UQ oxidoreductase. Indeed, our studies show this to be a reasonable possibility.

Ferredoxin

A ferredoxin is known to function as an electron-carrier component between the flavoprotein and cytochrome *P*-450 components of the electron-transport system for hydroxylation of steroids in many stereoidogenic organs, such as the adrenal cortex [21]. Adrenodoxin has been shown to be the major iron–sulphur protein in adrenocortical mitochondria, giving rise to a very intense EPR signal at 77 K and to be distinct from the iron–sulphur proteins comprising the mitochondrial respiratory chain (e.g. NADH dehydrogenase and SDH) [21]. Smith et al. [24] assigned an EPR signal at $g \sim 2.02, 1.94$ from the fat-body mitochondrial fraction of *M. sexta* to a ferredoxin; however, cytochrome *P*-450 was not detected, and a functional relationship between the two proteins, as part of the steroid-hydroxylation system of insect mitochondria, was not established. This is in contrast with our EPR results, where our analysis of the power-saturation characteristics (Figure 3a) of the $g \sim 2.02, 1.94$ signal detected from reduced preparations of *S. littoralis* fat-body mitochondrial membranes clearly suggests that the signal is more likely to be due to mitochondrial iron–sulphur proteins (e.g. NADH dehydrogenase and SDH).

However, the possibility that the signal from *S. littoralis* SMP reflects overlap from the [2Fe-2S] cluster of NADH dehydrogenase, SDH and a ferredoxin exists. Again, it is equally possible that the ferredoxin is present in concentrations too low to be resolved by EPR or that it may occur in the soluble matrix fraction, since, at least in adrenal cortex, it is only loosely bound to the mitochondrial membranes, being readily dissociated [44]. The matrix fraction does indeed display a signal characteristic of a ferredoxin at $g = 2.02, 1.94$, and the EPR characteristics of this signal strongly argue against it being due to membrane-detached SDH. No other proteins displaying a $g = 1.94$ signal in the reduced state normally occur in the soluble fraction. Furthermore, as no EPR signals assignable to the iron–sulphur proteins of the mitochondrial respiratory chain, in particular SDH, were observed from the matrix fraction, we propose that the $g = 2.02, 1.94$ signal represents detection of a cytochrome *P*-450-containing steroid-hydroxylation system similar to that of vertebrate adrenocortical mitochondria, with the EPR signal being due to a ferredoxin acting as an electron carrier between a flavoprotein and the cytochrome.

Finally, on the basis of immunoblot analyses, Chen et al. [27] have also proposed that *S. littoralis* fat-body ecdysone 20-monooxygenase may contain polypeptide components analogous to those in vertebrates; antibodies raised against the electron-transfer components of the bovine adrenocortical steroid-hydroxylation system revealed specific immunoreactive polypeptides in *S. littoralis* fat-body mitochondrial extracts and effectively inhibited ecdysone 20-mono-oxygenase activity. Consistent with this was the close correlation between developmental changes in mitochondrial ecdysone 20-mono-oxygenase activity and the abundance of polypeptides recognized by the anti-(cytochrome $P\text{-}450_{11b}$) and anti-(adrenodoxin reductase) antibodies. Whereas the approximate molecular masses of the latter polypeptides were reasonably close to those reported for the mammalian antigenic proteins, that of the polypeptide (73 kDa) detected with the anti-adrenodoxin antibody was considerably higher than that of its mammalian counterpart (12 kDa). The molecular basis of this observation requires clarification, but the possibility remains that a low-molecular-mass ferredoxin is present and awaits positive identification. As to the question of whether a ferredoxin is functionally involved in *S. littoralis* mitochondrial steroid hydroxylations, the answer must await further characterization of the overall organization of the electron-transfer chain, which will presumably involve further fractionation of fat-body mitochondria. Nevertheless, it is clear that the fat-body ecdysone 20-mono-oxygenase of *S. littoralis* provides a useful model for investigating both mitochondrial cytochrome *P*-450 steroid hydroxylase systems and insect respiratory systems.

We thank Mr. A. C. White for technical assistance with the EPR spectrometer. This work was financed by the Science and Engineering Research Council (Project Grant No. GR/F 18770 to H.H.R. and M.J.F.).

REFERENCES

1 Koolman, J. (ed.) (1989) Ecdysone: From Chemistry to Mode of Action, Thieme-Verlag, Stuttgart
2 Rees, H. H. (1989) in Ecdysone: From Chemistry to Mode of Action, (Koolman, J., ed.), pp. 152–160, Thieme-Verlag, Stuttgart
3 Redfern, C. P. F. (1989) in Ecdysone: From Chemistry to Mode of Action (Koolman, J., ed.), pp. 182–187, Thieme-Verlag, Stuttgart
4 Weirich, G. F., Svoboda, J. A. and Thompson, M. J. (1985) Arch. Insect Biochem. Physiol. **2**, 385–396
5 Smith, S. L. (1985) in Comprehensive Insect Physiology, Biochemistry and Pharmacology, vol. 7 (Kerkut, G. A. and Gilbert, L. I., eds.), pp. 295–341, Pergamon Press, Oxford
6 Cooper, D. Y., Schleyer, H., Estabrook, R. W. and Rosenthal, O. (1969) in Progress in Endocrinology (Gual, C. and Ebling, F. J. G., eds.), 784–802, Excerpta Medica, Amsterdam
7 Sih, C. J. (1969) Science **163**, 1297–1300
8 Lu, A. Y. H. and Levin, W. (1974) Biochim. Biophys. Acta **344**, 205–240
9 Gunsalus, I. C., Pedersen, T. C. and Sligar, S. G. (1975) Annu. Rev. Biochem. **44**, 377–407
10 Tchen, T. T. (1968) in Functions of the Adrenal Cortex, vol. 1 (McKerns, K. W., ed.), pp. 3–26, Appleton–Century–Crofts, New York
11 Mitani (1979) Mol. Cell. Biochem. **24**, 21–43
12 Hoggard, N. and Rees, H. H. (1988) J. Insect Physiol. **34**, 647–653
13 Omura, T., Sanders, E., Estabrook, R. W., Cooper, D. Y. and Rosenthal, O. (1966) Arch. Biochem. Biophys. **117**, 660–673
14 Kimura, T. and Suzuki, K (1967) J. Biol. Chem. **242**, 485–491
15 Katagiri, M., Ganguli, B. N. and Gunsalus, I. C. (1968) J. Biol. Chem. **243**, 3543–3546
16 Ortiz de Montellano, P. R. (ed.) (1986) Cytochrome *P-450*, Plenum, New York
17 Vermilion, J. L. and Coon, M. J. (1978) J. Biol. Chem. **253**, 8812–8819
18 Estabrook, R. W., Peterson, J., Baron, J. and Hildebrandt, A. (1972) in Methods in Pharmacology (Chignell, C. F., ed.), vol. 2, pp. 303–350, Appleton–Century–Crofts Educational Division, Meredith Corporation, New York
19 Murakami, K. and Mason, H. S. (1967) J. Biol. Chem. **242**, 1102–1110
20 Tsai, R., Yu, C. A., Gunsalus, I. C., Peisach, J., Blumberg, W. E., Orme-Johnson, W. H. and Beinert, H. (1970) Proc. Natl. Acad. Sci. U.S.A. **66**, 1157–1163
21 Estabrook, R. W., Suzuki, K., Mason, J. I., Baron, J., Taylor, E. E., Simpson, E. R., Purvis, J. and McCarthy, J. (1973) in Iron–Sulfur Proteins: Biological Properties (Lovenberg, W., ed.), vol. 1, pp. 193–223, Academic Press, New York and London

22 Beinert, H. (1978) Methods Enzymol. **54**, 133–150
23 Ohnishi, T. (1979) in Membrane Proteins of Energy Transductions (Capaldi, R. H., ed.), pp. 1–87, Marcel Dekker, New York
24 Smith, S. L., Bollenbacher, W. E. and Gilbert, L. I. (1980) in Progress in Ecdysone Research (Hoffmann, J. A., ed.), pp. 139–162, Elsevier, Amsterdam
25 Weirich, G. F., Svoboda, J. A. and Thompson, M. J. (1984) in Biosynthesis, Metabolism and Mode of Action of Invertebrate Hormones (Hoffmann, J. and Porchet, M., eds.), pp. 227–233, Springer-Verlag, Berlin
26 Smith, S. L., Bollenbacher, W. E., Cooper, D. Y., Schleyer, H., Wielgus, J. J. and Gilbert, L. I. (1979) Mol. Cell. Endocrinol. **15**, 111–133
27 Chen, J.-H., Hara, T., Fisher, M. J. and Rees, H. H. (1994) Biochem. J. **299**, 711–717
28 Kearney, E. B., Ackrell, B. A. C., Mayr, M. and Singer, T. P. (1974) J. Biol. Chem. **249**, 2016–2020
29 Shergill, J. K. and Cammack, R. (1994) Biochim. Biophys. Acta **1185**, 43–49
30 Cammack, R. (1988) Methods Enzymol. **167**, 427–436
31 Albracht, S. P. J., Van Verseveld, H. W., Hagen, W. R. and Kalkman, M. J. (1980) Biochim. Biophys. Acta **593**, 173–186
32 Ruzicka, F. J. and Beinert, H. (1977) J. Biol. Chem. **252**, 8440–8445
33 Johnson, M. K., Morningstar, J. E., Oliver, M. and Frermen, F. E. (1987) FEBS Lett. **226**, 129–133
34 Ohnishi, T., Lim, J., Winter, D. B. and King, T. E. (1976) J. Biol. Chem. **251**, 2105–2109
35 Maguire, J. J., Johnson, M. K., Morningstar, J. E., Ackrell, B. A. C. and Kearney, E. B. (1985) J. Biol. Chem. **260**, 10909–10912
36 Hatefi, Y., Haavik, A. G. and Griffiths, D. E. (1962) J. Biol. Chem. **237**, 1680–1685
37 Ohnishi, T., Wilson, D. F., Asakura, T. and Chance, B. (1972) Biochem. Biophys. Res. Commun. **46**, 1631–1638
38 Albracht, S. P. J. (1974) Biochim. Biophys. Acta **347**, 183–192
39 Williams-Smith, D. L. and Patel, K. (1975) Biochim. Biophys Acta **405**, 243–252
40 de Duve, C. (1983) Sci. Am. **248**, 74–84
41 Salerno, J. (1984) J. Biol. Chem. **259**, 2331–2336
42 Aasa, R., Albracht, S. P. J., Falk, K.-E., Larn, B. and Vanngard, T. (1976) Biochim. Biophys. Acta **422**, 260–272
43 Ohnishi, T., Schägger, H., Meinhardt, S. W., LoBrutto, R., Sink, T. and von Jagow, G. (1989) J. Biol. Chem. **264**, 735–744
44 Kimura, T., Parcells, J. H. and Wang, H.-P. (1978) Methods Enzymol. **52**, 132–142
45 Ruzicka, F. J. and Beinert, H. (1978) J. Biol. Chem. **253**, 2514–2517
46 Orme-Johnson, N. R., Hansen, R. E. and Beinert, H. (1974) J. Biol. Chem. **249**, 1928–1939
47 Flatmark, T., Ruzicka, F. J. and Beinert, H. (1976) FEBS Lett. **63**, 51–55
48 Trumpower, B. L. (1981) J. Bioenerg. Biomembr. **13**, 1–24

Received 29 September 1994/9 December 1994; accepted 19 December 1994